Precisely Controlled Anodic Etching for Processing of GaAs-based Quantum Nanostructures and Devices

Nanako Shiozaki, Taketomo Sato, Masamichi Akazawa and Hideki Hasegawa

Research Center for Integrated Quantum Electronics and Graduate School of Information Science and Technology, Hokkaido University, N-13, W-8, Sapporo 060-8628, Japan.

Abstract. For controlled low-damage etching of AlGaAs/GaAs nanostructures, fundamental properties of an etching process consisting of anodic oxidation and subsequent oxide dissolution are investigated both theoretically and experimentally. Anodic oxides formed on GaAs (001) and (111)B surfaces have the same composition and the same anodization parameters according to XPS, SEM and AFM measurements. The same applies to those formed on $Al_{0.3}Ga_{0.7}As$ (001) and (111)B surfaces. The etching depth can be precisely controlled in nanometer scale by the anodization voltage. Selective etching was realized, using the lithography patterns. The surface morphology is much better than that in the standard wet chemical etching.

1. INTRODUCTION

In the III-V semiconductor technology, wet chemical etching in acid solutions is widely used in various steps of device fabrication due to its low damage nature. Additionally, recent progress of III-V quantum nanotechnology has revealed importance of other surfaces such as (111), (311), (411) and (521) surfaces, and controlled etching of these surfaces is important in addition to the conventional (001) surfaces. For example, quantum nanostructure fabrication by MBE or MOVPE growth on pre-patterned substrates requires wet etching for fabrication of initial patterns with various facets. However, precise control of the etching depth is extremely difficult in the nanometer length scale, because the etch rate is very sensitive to temperature variation and local fluctuation of the etchant composition.

Recently, our group reported on anodic etching of n-type InP, using the active dissolution mode in the HCl-based electrolyte [1,2]. In this low energy processing, the etching depth can be precisely controlled by the total charge based on the Faraday's law. Using a pulsed mode, an extremely small etching rate of about 10^{-5} nm per pulse has been achieved. However, there are some problems. One is unexpected occurrence of active-passive transition which leads formation of nonuniform porous structures [2]. Another problem is that etching rate may be enhanced or reduced at corners by current crowding or spreading. Additionally, the etching rate will depend strongly on the orientation of the surface, making uniform etching of a nanostructure difficult. An alternative anodic etching method is to form an anodic oxide film and subsequently dissolve it in a different solution. Recently, we applied this to MBE-grown GaAs/AlGaAs ridge quantum wires [3].

The purpose of this paper is to investigate the basic properties of an etching process consisting of anodic oxidation and subsequent oxide dissolution for (001) and (111)B AlGaAs/GaAs surfaces. Anodic oxidation of (111)B is reported for the first time.

2. A SIMPLE THEORY OF ANODIC OXIDE FORMATION

We assume a simple set-up shown in **Fig.1**. When the anodization voltage is turned on, the current rises up very sharply as the GaAs substrate dissolves into the electrolyte in the form of oxides (active dissolution). However, by use of a suitable electrolyte, dissolution is stopped due to a diffusion barrier in the electrolyte, and growth of a solid-state oxide film consisting of Ga oxide and As oxide is initiated after the passivation time, t_p. This is called active-passive transition. As the oxide layer becomes thicker on the surface, the current decreases exponentially, since the voltage required for transport of ionic species through the oxide layer increases in proportion to the oxide thickness. Finally, a balance is reached between formation of oxide and dissolution of oxide. By applying the Faraday's law, the following equation for anodization current density $J(t)$ is derived.

$$J(t) = (J_0 - J_f)\mathrm{e}^{-\frac{t-t_p}{\tau}} + J_f \qquad (1a)$$

where $$J_0 = \frac{V_a - V_r}{(R_e + R_0)S}, \quad J_f = \frac{xFd_s v_{ds}}{M_s \kappa} \quad \text{and} \quad \tau = \frac{xFd_s S}{M_s \kappa E_{ox}}\left(R_0 + R_e\right) \qquad (1b)$$

Here, we assume that the electric field, E_{ox}, for ion transport through the anodic oxide is constant, and that simultaneous dissolution of oxide takes place on the oxide surface at velocity of v_{ds}. J_0 and J_f are the initial and final current density, respectively. V_a, V_r, R_e, R_o and S are the anodization voltage, the rest potential at the semiconductor/electrolyte interface, the external resistance, the other series resistance due to electrolyte and semiconductor bulk and the anode area, respectively. F, M_s, d_s and x are Faraday's constant (96,485.3 C/mol), the molecular weight of semiconductor, the density of semiconductor and the number of holes required to etch one molecule of semiconductor, respectively. κ is the ratio of the oxide thickness to the thickness of the semiconductor consumed for oxidation. κ is larger than unity due to inclusion of oxygen atoms in the oxide layer.

Thus, an exponentially decaying behavior of current is expected, as schematically shown in the inset of **Fig.2.** Then, the thickness of the semiconductor, T_s, which has undergone anodic reaction during the anodization time, t, is given by the following equation for the case of $exp(-(t-t_p)/\tau) \ll 1$.

$$T_s(t) = \frac{1}{\kappa E_{ox}}\left\{\frac{t_p}{\tau} + 1\right\}\left(V_a - V_r\right) + \frac{v_{ds}}{\kappa}\left(t - t_p - \tau\right) \qquad (2)$$

Thus, if the conditions of $t_p \ll \tau$ and $J_f \ll J_0$ hold, t_p/τ in the first term as well as the second term can be ignored so that the etching thickness is precisely controlled by the anodization voltage.

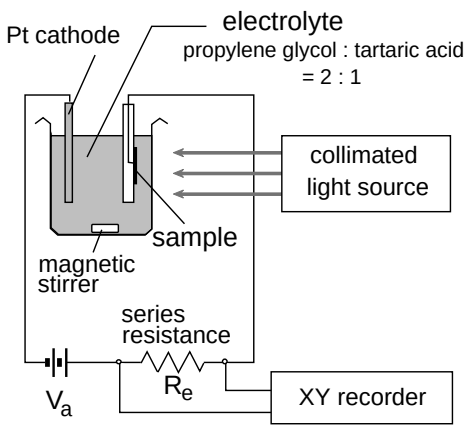

Fig.1 Anodization set-up.

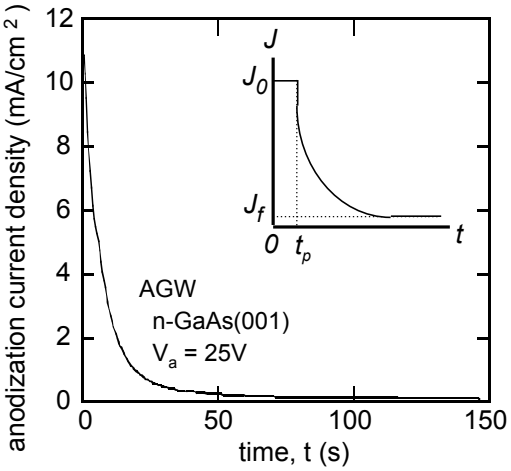

Fig.2 Measured behavior of anodization current density with a theoretical behavior in inset.

3. EXPERIMENTAL STUDY AND DISCUSSION

3.1 Anodic oxidation behavior and parameters

The electrochemical cell shown in **Fig.1** was used. Holes required for anodization were generated by the light illumination using a tungsten lamp. n-GaAs (001) and (111)B substrates with a carrier density of n=1x10^{18} cm^{-3} and n-$Al_{0.3}Ga_{0.7}As$ layers with a carrier density of n=8x10^{16} cm^{-3} grown on n-GaAs (001) and (111)B substrates were used. For the current supply, GeAu/Ni ohmic contacts were formed on the backside of substrates. A mixed solution of propylene glycol and tartaric acid solution (AGW electrolyte [4]) with propylene glycol : tartaric acid = 2:1 was used as the electrolyte. It avoids large dissolution of the oxide during anodization. After anodization, the oxide film was carefully dissolved by immersing into a HCl solution.

Properties of oxides and etched surfaces were characterized using scanning electron microscopy (SEM), atomic force microscopy (AFM), ellipsometry and X-ray photoelectron spectroscopy (XPS) techniques. Ellipsometry data were taken by using a He-Ne laser ($\lambda = 632.8$ nm) and the data were analyzed by using the published optical properties of GaAs and AlGaAs [5]. Measurements of oxide thickness and etched semiconductor thickness by AFM were carried out on lithographically defined line and space patterns for selective anodic oxidation. A monochromatic AlKα (1486.6 eV) radiation was used as the X-ray source for XPS measurements. The binding energies of core level peaks were corrected with respect to the C1s position at 285.0 eV.

Figure 2 shows a typical transient curve of the anodic current vs. time measured on the n-GaAs (001) electrode. The behavior agrees with Eq.(1a) with $t_p = 0$ and $J_f = 0$. Thus, the result indicates a nearly ideal case where the passivation time and oxide dissolution can be ignored.

The thickness of anodic oxides, T_{ox}, and the etching depth after removal of the oxide films, T_s, are plotted in **Figs. 3(a) and (b)** as a function of the anodization voltage, V_a, for n-GaAs and n-$Al_{0.3}Ga_{0.7}As$, respectively. In both cases, oxide thicknesses were the same for (001) and (111)B substrates, and showed a linear relation to V_a, with standard deviations of 2.71nm and 2.36nm for n-GaAs and n-$Al_{0.3}Ga_{0.7}As$, respectively. The measured average oxidation rate per volt given by E_{ox}^{-1} is 2.0 nm/V for (001) and (111)B GaAs, and 1.8 nm/V for (001) and (111)B $Al_{0.3}Ga_{0.7}As$. The value of 2.0 nm/V for (001) GaAs surface was in good agreement with the previous study [4], although the previous study was carried out in a much larger oxide thickness range. Since E_{ox} related to ion transport is expected to be sensitive to oxide composition, the fact that slopes are the same for (001) and (111)B surfaces strongly suggests that the same oxides are formed on both surfaces in spite of difference of the bond density on the surface. This feature seems to be very attractive for etching of the structures having both (001) and (111)B facets where both facets are etched by an equal thickness. It is also likely that the same oxides are formed on other high index surfaces.

The etching depth, T_s, showed also linear relation to the anodization voltage, indicating that dissolution of anodic film during anodization is negligible according to Eq.(2). The etching depth was smaller than the oxide thickness, since oxide films became thicker than the semiconductor by a factor of $\kappa > 1$. From experiments, κ for GaAs is 1.8 and κ for $Al_{0.3}Ga_{0.7}As$ is 1.4.

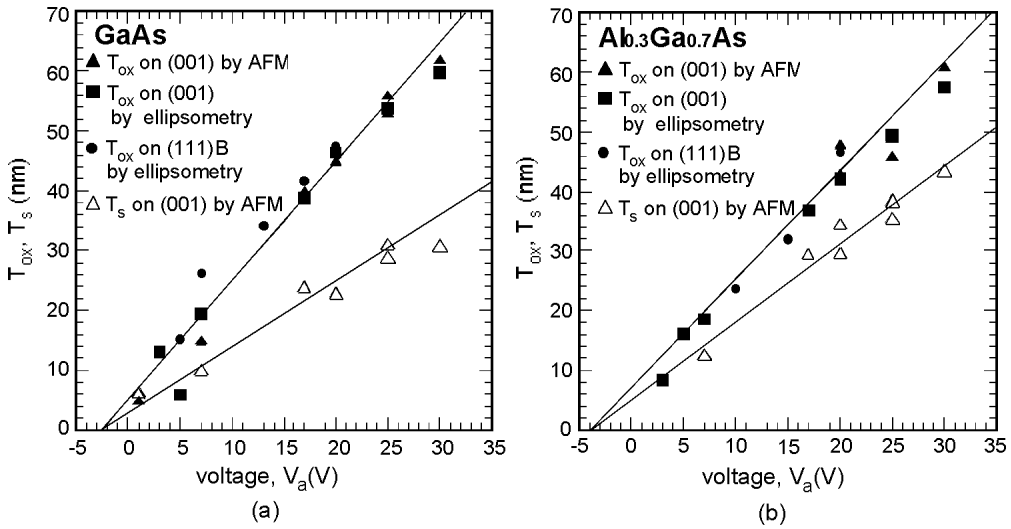

Fig.3 Measured oxide thickness, T_{ox}, and the etched semiconductor thickness, T_s for (a) (001) and (111)B GaAs surfaces and (b) (001) and (111)B $Al_{0.3}Ga_{0.7}As$ surfaces.

3.2 XPS analysis of anodic oxides

Figure 4 shows the measured XPS spectra data for AlGaAs. The binding energies for oxide peaks are in good agreement with the reported data [6] within experimental errors. Thus, As3d, Ga3d and Al2p core levels observed on 50 nm thick oxides on GaAs and AlGaAs were assigned to As_2O_3, Ga_2O_3, and Al_2O_3 respectively for both of (001) and (111)B orientations. It is seen that XPS spectra from (001) and (111)B surfaces completely overlap without any appreciable difference in the binding

energy and the peak shape. This again confirms that the same oxide is formed on two surfaces. Thus, the anodic reaction taking place at the anode is the following for $x = 0$ and $x = 0.3$.

$$Al_xGa_{1-x}As + 6OH^- + 6h^+ = \frac{1}{2}\left(x\,Al_2O_3 + (1-x)Ga_2O_3\right) + \frac{1}{2}As_2O_3 + 3H_2O \qquad (3)$$

3.3 Selective etching experiment

For the application of the anodic etching to the nano fabrication process, the etching shape or the surface morphology are very important factors as well as the controllability of the etching depth. As shown in **Fig.5** by a plan view of a GaAs (001) sample after selective anodic etching at $V_a = 25$V, selective etching using the photo-resist mask produced a pattern which precisely follows the mask pattern with an etching depth of 29-31nm. Furthermore, the AFM observation showed that the morphology of the surface was considerably better than that after a standard wet and dry etching process. The rms roughness was found to be below 1.0 nm. These results indicate that the anodic process seems to be very useful for the formation of nanostructures without size fluctuation and a processing damage. Although it is not investigated here, the ultrathin anodic oxide grown here may also be useful for surface passivation by further annealing etc. Although thick oxides are known to be rather poor for such a purpose, it is possible that the situation may be different in the nanoscale regime.

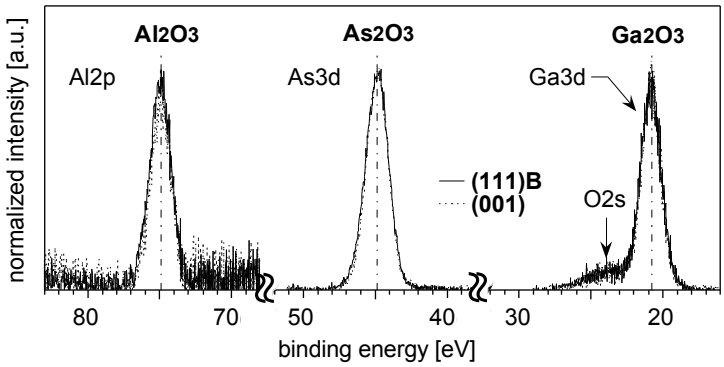

Fig.4 XPS core level spectra from (001) and (111)B $Al_{0.3}Ga_{0.7}As$ surfaces.

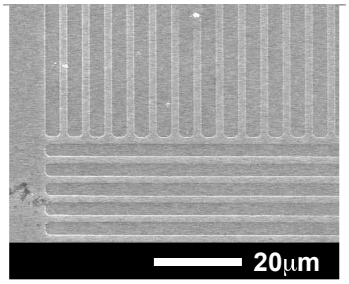

Fig.5 A plan view of a sample after selective anodic etching at $V_a = 25$V using a photo-resist mask.

4. CONCLUSION

For controlled etching of AlGaAs/GaAs nanostructures, fundamental properties of an etching process consisting of anodic oxidation and subsequent oxide dissolution were investigated both theoretically and experimentally. Anodic oxides formed on GaAs (001) and (111)B surfaces have the same composition and the same anodization parameters. The same applies to those formed on $Al_{0.3}Ga_{0.7}As$ (001) and (111)B surfaces. The etching depth can be precisely controlled in nanometer scale by the anodization voltage. Selective etching was realized, using the lithography patterns. The surface morphology was much better than that in the standard wet chemical etching.

Acknowledgments: This work is supported partly by 21 Century COE program, "Meme-media Technology Approach to the R&D of next-generation ITs," from MEXT, Japan.

References

[1] C. Kaneshiro, T. Sato and H. Hasegawa, Jpn. J. Appl. Phys. **38** (1999) pp. 1147-1152.
[2] H. Hasegawa and T. Sato, Electrochemica Acta **50** (2005) pp. 3015-3027.
[3] N. Shiozaki, T. Sato and H. Hasegawa, J. Vac. Sci. Technol. **B23** (2005) pp.1714-1721.
[4] H. Hasegawa and H. L. Hartnagel, J.Electrochem.Soc. **123**(1976) pp. 713-723.
[5] D. E. Aspnes, B. Schwartz, A. A. Studna, L. Derick and L. A. Koszi, J. Appl. Phys. **48** (1977) pp. 3510-3513.
[6] J. Shin, K. M. Geib, C. W. Wilmsen, P. Chu and H. H. Wieder, J. Vac. Sci. Technol. **A9** (1991) pp.1029-1034.